Supporting Information

Composition effects on exciton recombination dynamics of blue-emitting alloyed $Cd_{1-x}Zn_xS/ZnS$ quantum dots

Wenzhi Wu[†, *, 1], Weilong Liu[†, *, 2], Qiuju Han [3], Yachen Gao [1], Degui Kong [1], Qingxin Yang[2]

[1] School of Electronic Engineering, Heilongjiang University, Harbin, Heilongjiang, 150030, China

[2] School of Physics, Harbin Institute of Technology, Harbin, Heilongjiang, 150001, China

[3] School of Arts and Sciences, Northeast Agricultural University, Harbin, Heilongjiang, 150030, China

[†] Wenzhi Wu and Weilong Liu contributed equally to this work

[*] wuwenzhi@hlju.edu.cn and liuwl@hit.edu.cn

Contents

S1. Temperature-dependent steady-state PL spectral contours

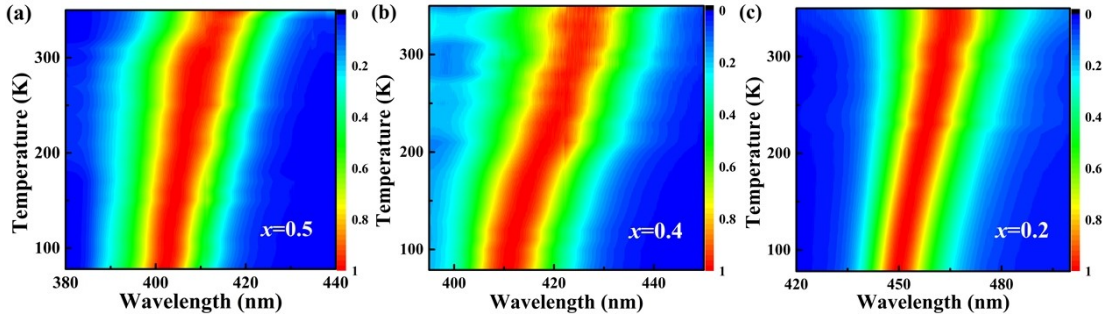

Fig. S1. (a)-(c) Steady-state PL spectral contours of $Cd_{1-x}Zn_xS/ZnS$ QDs (x=0.5, 0.4, and 0.2) measured at the temperatures range from 80 to 350 K.

S2. Time-resolved PL dynamics at representative temperatures

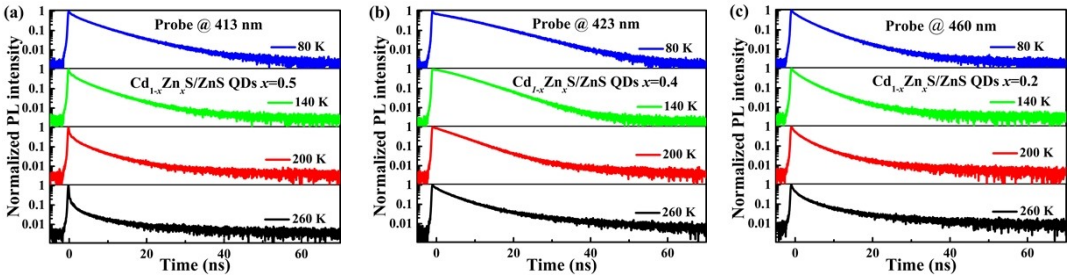

Fig. S2. (a)-(c) Time-resolved PL dynamics of $Cd_{1-x}Zn_xS$ /ZnS QDs (x=0.5, 0.4, and 0.2) at 80, 140, 200, 260 K probed at corresponding emission peaks.

S3. The decay-associated spectra of $Cd_{0.7}Zn_{0.3}S/ZnS$ QDs

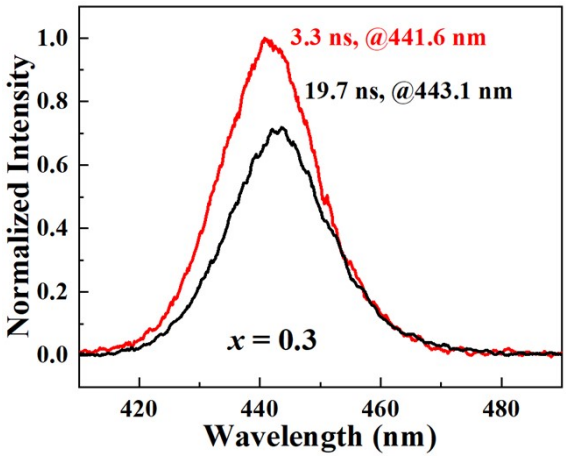

Fig. S3. The decay-associated spectra, as well as the peak positions and lifetimes, of the $Cd_{0.7}Zn_{0.3}S/ZnS$ QDs obtained from ns time-resolved PL spectra.

We didn't measure the ns time-resolved PL spectra of the x=0.4 and 0.5 $Cd_{1-x}Zn_xS/ZnS$ QDs. The excitonic state lifetimes of the x=0.4 and 0.5 QDs are quite similar as the time resolution of the intensified CCD (ICCD) detector (~2 ns), and the PL peaks are too close to the excitation light (400 nm), so the fast components are seriously

disturbed by excitation light and the reliable exciton lifetime cannot be obtained in our ns time-resolved PL measurements using ICCD. Thus, we analyzed the average PL lifetimes measured by the time-correlated single photon counting (TCSPC) system in Fig. 3d, the IRF of the TCSPC system is ~0.2 ns.

S4. Exciton number and absorption cross-section estimation

We use the method provided by Lian [1] and Jiang [2] for estimating the average exciton number in QDs. With a usual assumption, TA signal can be described by the state-filling effect, and the number of excitons per QD generated by the excitation pulse is assumed to obey a Poisson distribution [3]

$$P_n(w) = \frac{w^n}{n!}e^{-w} \tag{1}$$

where $P_n(w)$ is the probability of having QDs with n excitons when the average number of excitons per QD is w. In the case of short-pulse excitation, we can calculate w as a product of the per-pulse fluence measured in photons per centimeter squared (j_p) and the QDs absorption cross-section at the pump wavelength (σ_a), $w = j_p\sigma_a$.

The average number of excitons per QD can be quantified by examining the photoinduced bleach signals as a function of excitation power. Due to the double degeneracy of the lowest emission level for II-VI type-I QDs [2, 4], the amplitudes of normalized PB signals are given by [5]

$$\Delta S_{t_0} = 2 - (2 + w)e^{-w} \tag{2}$$

$$\Delta S_{t_L} = 1 - e^{-w} \tag{3}$$

where ΔS_{t_0} is the normalized bleach signal at t_0, when no exciton decay has occurred, and ΔS_{t_L} is the normalized bleach signal at t_L, when the biexciton states have decayed to single exciton states and there is negligible decay of single exciton states. We use the pump fluence dependences of the normalized bleach signal amplitudes at $t_0 = 1$ ps, and $t_L = 1$ ns to fit the average number of excitons per QD w. The fitting results are shown in Fig. S4. The obtained absorption cross-section at 400 nm for $Cd_{0.8}Zn_{0.2}S/ZnS$ and $Cd_{0.7}Zn_{0.3}S/ZnS$ QDs are ~2.1×10^{-15}cm^2 and ~1.8×10^{-15}cm^2, respectively.

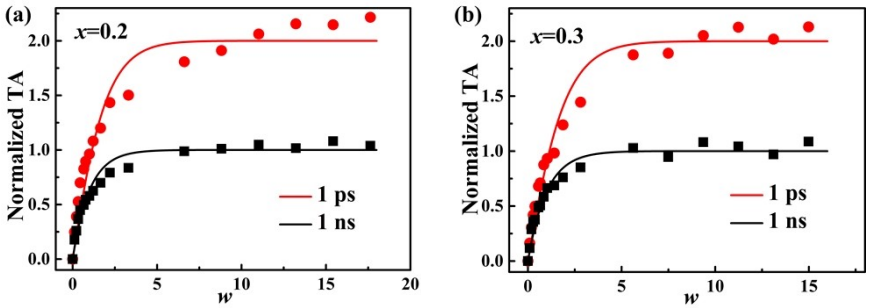

Fig. S4. Normalized transient photoinduced bleach signals for ΔS_{t_0} (red circles) and ΔS_{t_L} (black squares) in (a) $Cd_{0.8}Zn_{0.2}S/ZnS$ and (b) $Cd_{0.7}Zn_{0.3}S/ZnS$ QDs as a function of average number of excitons per QD. The solid lines are fits according to the model described above.

S5. Transient absorption 2D contours at representative pump fluences

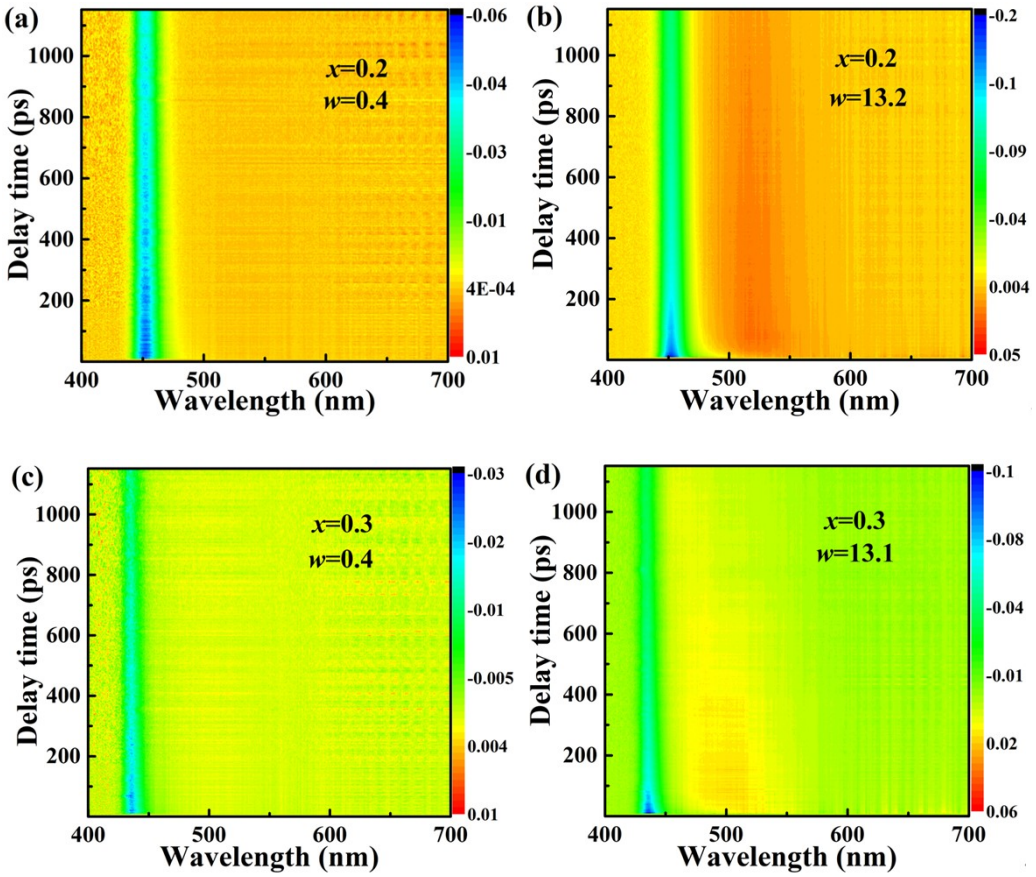

Fig. S5. The spectral 2D contours of (a) (b) $Cd_{0.8}Zn_{0.2}S/ZnS$ and (c) (d) $Cd_{0.7}Zn_{0.3}S/ZnS$ QDs at representative low and high pump fluences.

S6. Transient absorption spectra of $Cd_{0.7}Zn_{0.3}S/ZnS$ QDs at representative pump fluences

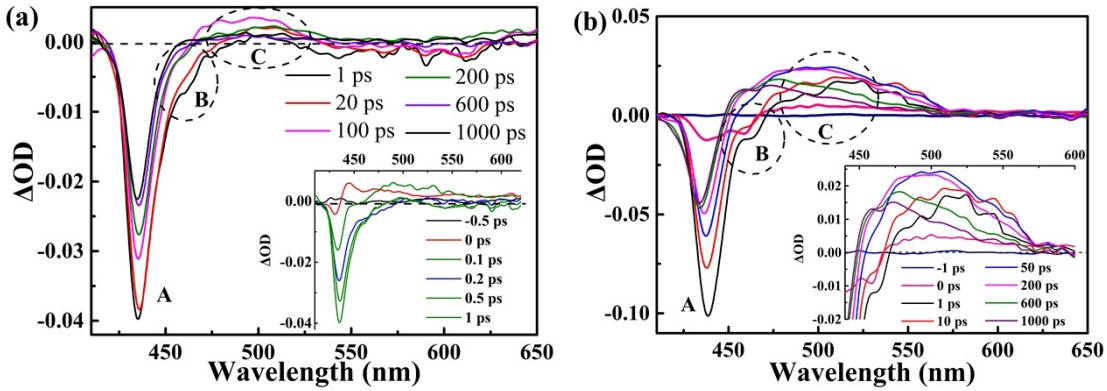

Fig. S6. Transient absorption spectra of $Cd_{0.7}Zn_{0.3}S/ZnS$ QDs at different delay time at (a) low (w=1.0) and (b) high (w=15.0) pump fluences. The inserts in panel (a) and (b) show the TA spectra before and after 1 ps, respectively.

S7. The non-normalized dynamics probed at the PB and PA regions

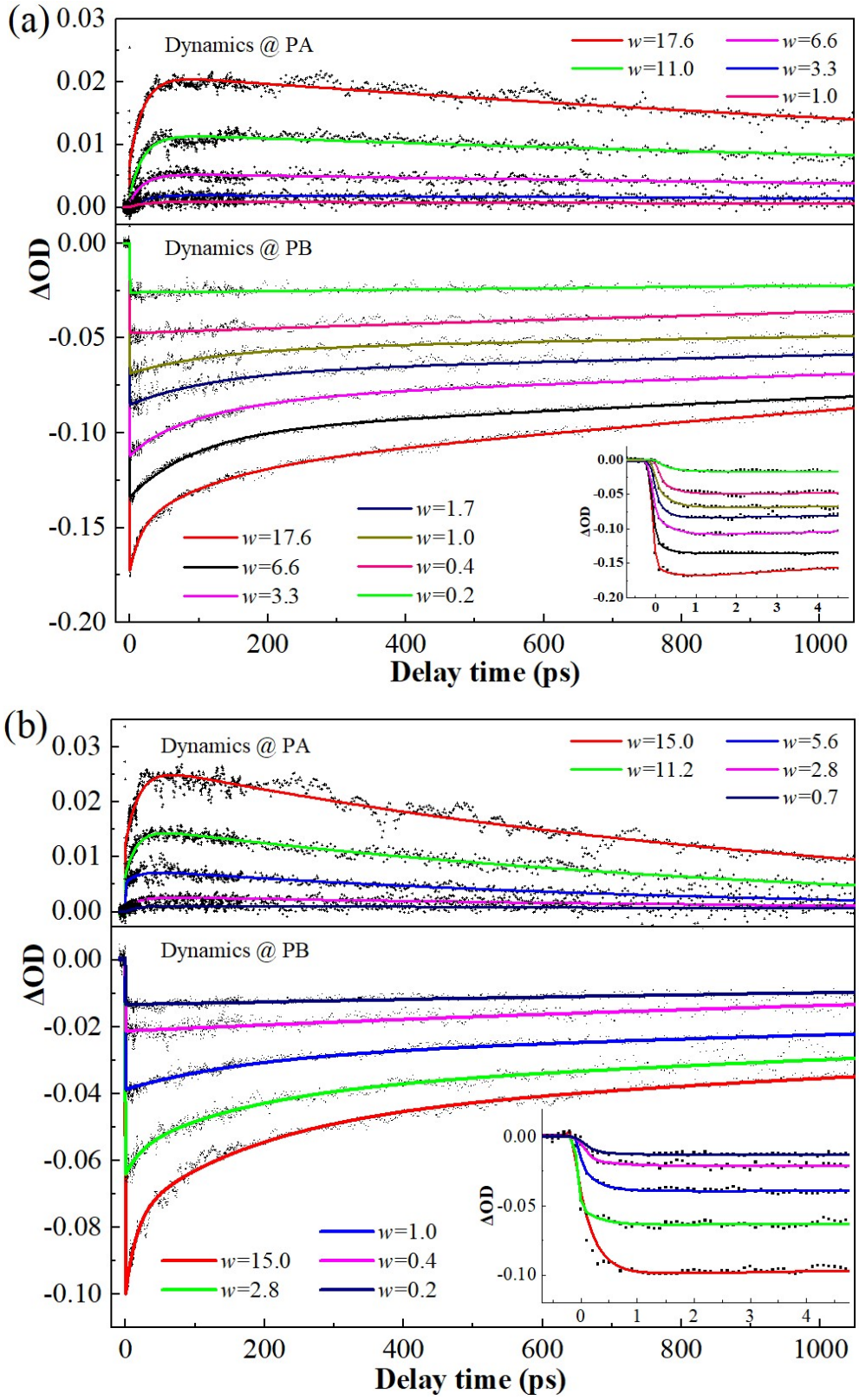

Fig. S7. Dynamics of (a) $Cd_{0.8}Zn_{0.2}S/ZnS$ and (b) $Cd_{0.7}Zn_{0.3}S/ZnS$ QDs probed at PB and PA regions under different pump fluences. The inserts shows the rising edge of the dynamics.

S8. The maximum at PB and PA regions under different pump fluences

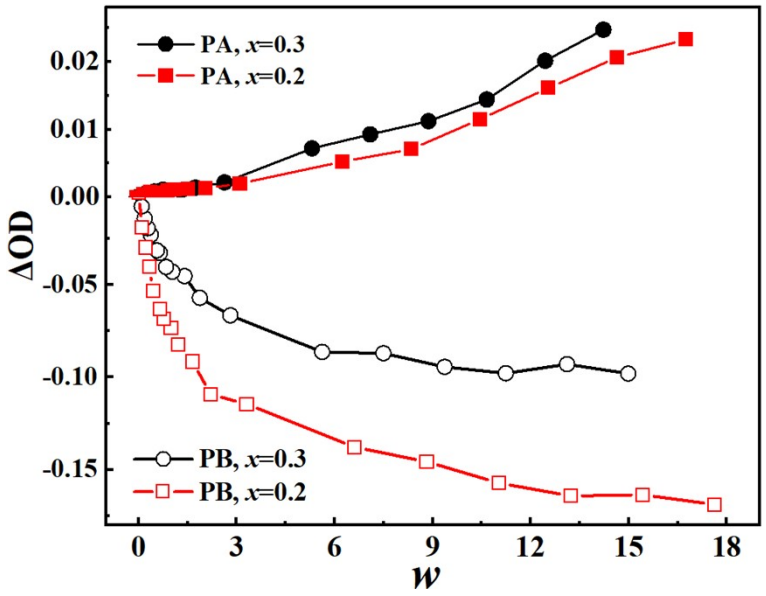

Fig. S8. The maximum at PB and PA regions as a function of average number of excitons per QD, *w*.

S9. Fitting parameters for the photoinduced bleach dynamics of $Cd_{1-x}Zn_xS/ZnS$ QDs

Table S1. Fitting parameters for the photoinduced bleach dynamics of $Cd_{0.8}Zn_{0.2}S/ZnS$ and $Cd_{0.7}Zn_{0.3}S/ZnS$ QDs excited to different average number of excitons per QD, *w*.

	w	τ_1, ps (A_1, %)	τ_2, ps (A_2, %)	τ_3, ps (A_3, %)
	17.6	(71)	103 (17)	15 (12)
	15.4	(70)	126 (18)	18 (12)
	13.2	(69)	130 (20)	20 (11)
	11.0	(71)	138 (19)	25 (10)
	8.8	(72)	131 (20)	23 (8)
	6.6	(72)	132 (21)	26 (7)
	3.3	(73)	130 (22)	30 (5)
	2.2	(81)	112 (19)	(0)
$Cd_{0.8}Zn_{0.2}S/ZnS$	1.7	>>1 ns (80)	125 (20)	(0)
	1.2	(83)	118 (17)	(0)
	1.0	(82)	120 (18)	(0)
	0.8	(82)	131 (18)	(0)
	0.7	(100)	(0)	(0)
	0.4	(100)	(0)	(0)
	0.3	(100)	(0)	(0)
	0.2	(100)	(0)	(0)
	0.1	(100)	(0)	(0)
	15.0	(49)	180 (20)	18 (31)
$Cd_{0.7}Zn_{0.3}S/ZnS$	13.1	>>1 ns (47)	185 (30)	16 (23)
	11.2	(56)	169 (22)	17 (22)

	9.4		(56)	175	(25)	19	(19)
	7.5		(62)	170	(20)	21	(18)
	5.6		(58)	170	(29)	25	(13)
	2.8		(62)	168	(27)	23	(11)
	1.9		(71)	155	(29)		(0)
	1.4		(74)	165	(26)		(0)
	1.0		(75)	181	(25)		(0)
	0.8		(76)	177	(24)		(0)
	0.7		(100)		(0)		(0)
	0.6		(100)		(0)		(0)
	0.4		(100)		(0)		(0)
	0.3		(100)		(0)		(0)
	0.2		(100)		(0)		(0)

References

1. K. Wu, G. Liang, Q. Shane, Y. Ren, D. Kong, and T. Lian, "Ultrafast Interfacial Electron and Hole Transfer from $CsPbBr_3$ Perovskite Quantum Dots," Journal of the American Chemical Society **137**, 12792-12795 (2015).
2. K. Wei, X. Zheng, X. Cheng, C. Shen, and T. Jiang, "Observation of Ultrafast Exciton-Exciton Annihilation in $CsPbBr_3$ Quantum Dots," Advanced Optical Materials **4**, 1993-1997 (2016).
3. V. I. Klimov, "Spectral and dynamical properties of multilexcitons in semiconductor nanocrystals," Annual Review of Physical Chemistry **58**, 635-673 (2007).
4. V. I. Klimov, A. A. Mikhailovsky, S. Xu, A. Malko, J. A. Hollingsworth, C. A. Leatherdale, H. Eisler, and M. G. Bawendi, "Optical gain and stimulated emission in nanocrystal quantum dots," Science **290**, 314-317 (2000).
5. J. Huang, Z. Huang, Y. Yang, H. Zhu, and T. Lian, "Multiple Exciton Dissociation in CdSe Quantum Dots by Ultrafast Electron Transfer to Adsorbed Methylene Blue," Journal of the American Chemical Society **132**, 4858-4864 (2010).